Available online at www.sciencedirect.com
SCIENCE DIRECT®
Physica C 426–431 (2005) 1585–1590
PHYSICA C
www.elsevier.com/locate/physc

Detection of micro-flaws on thin copper tubes using SQUID-NDI system based on eddy current technique

Y. Hatsukade [a,*], A. Kosugi [a], K. Mori [b], S. Tanaka [a]

[a] *Department of Ecological Engineering, Toyohashi University of Technology, 1-1 Hibarigaoka, Tempaku-cho, Toyohashi, Aichi 441-8580, Japan*
[b] *Sumitomo Light Metal Industries, Ltd. Copper Works, 100 Ougishinmichi, Ichinomiya-cho, Hoi-gun, Aichi 441-1295, Japan*

Received 23 November 2004; accepted 7 February 2005
Available online 19 July 2005

Abstract

We constructed a SQUID-NDI system for inspection of micro-flaws on heat exchanger copper tubes employing HTS-SQUID gradiometer and Helmholtz-coil-type inducer. The HTS-SQUID gradiometer was cooled using a coaxial pulse tube cryocooler. The detection of artificial flaws several tens of μm in depth on copper tubes, 6.35 mm in outer diameter and 0.825 mm in thickness, was demonstrated using the SQUID-NDI system. With excitation field of 1.6 μT at 5 kHz, the system could detect a 30-μm-depth flaw with SN ratio of about 20, where conventional NDI methods should fail to detect. The amplitude of the magnetic signal due to the flaw was in proportion to the square of flaw depth. Taking into account of the system's noise level, the results suggest that the SQUID-NDI system has a potential to detect sub-10-μm-depth flaws on copper tubes.

PACS: 85.25; 81.70

Keywords: HTS-SQUID; Nondestructive inspection; Copper tube; Cryocooler

1. Introduction

In recent years, the thickness of heat exchanger tubes has tended to be decreased to obtain better heat exchange efficiency. Thus, in the case of thin heat exchanger copper tube less than 1 mm in thickness, even a shallow flaw 20–30 μm in depth on surface can be a potential cause of the tube breakage when the tube is in bending or flaring processes. Therefore, nondestructive inspection (NDI) technique for quality control on the copper tubes requires higher sensitivity than ever. Eddy current testing (ECT) has been employed for detection of flaws on copper tubes in tube factories [1–3].

* Corresponding author. Tel.: +81 532 44 1282; fax: +81 532 44 6926.
E-mail address: hatukade@eco.tut.ac.jp (Y. Hatsukade).

0921-4534/$ - see front matter © 2005 Elsevier B.V. All rights reserved.
doi:10.1016/j.physc.2005.02.123

However, the minimum detectable depth by commercial ECT systems is 50–100 μm. Thus, more sensitive NDI technique for the copper tubes than the conventional methods is in strong demand.

High temperature superconductor (HTS) superconducting quantum interference device (SQUID) is an extreme sensitive sensor with magnetic field resolution of several tens $fT/Hz^{1/2}$ [4]. Due to its great sensitivity up to several hundreds kHz, NDI using HTS-SQUID is a superior technique to the ECT concerning detection of small defects [5–7]. However, it is supposed that NDI technique for heat exchanger copper tubes must be executed in possibly magnetically noisy tube factory by manufacturers. Thus, the NDI technique requires not only sensitivity but also robustness against noise and easy handling.

To meet the requests, we constructed a NDI system for inspection of micro-flaws on heat exchanger copper tubes employing an HTS-SQUID gradiometer and a cryocooler. The principle of this NDI is based on eddy current technique, and a Helmholtz-coil-type inducer is used. In this paper, the details of the system and demonstration of detection of surface flaws, several tens μm in depth, on thin heat exchanger copper tubes are described.

2. Experimental

2.1. Specimens

Heat exchanger copper tubes that had artificial shallow flaws with various depths on surfaces were prepared as specimens. These tubes were selected from commercial products. The dimensions of all the tubes are 6.35 mm in outer diameter, 0.825 mm in thickness and 300 mm in length. The common dimensions of the flaws are 100 μm in width and 15 mm in length. The depths of the flaws are 100 μm, 50 μm, and 30 μm, respectively. The flaws were made using an electric discharge machine.

2.2. SQUID-NDI system

A SQUID-NDI system for inspection of heat exchanger copper tubes was constructed in an eddy-current shielded room. A Helmholtz-coil-type inducer was employed to induce eddy current in the tubes [8]. During the processes of making a thin copper tube, a flaw on the tube is lengthened toward the axis of tube, and also thinned. For detection of such long and shallow flaws, a Helmholtz-coil-type inducer is suitable since it induces an eddy current flowing along the circumference of the tube (perpendicular to the axis of tube) when the tube is passed through the inducer. The principle of the eddy current based SQUID-NDI technique is schematically illustrated in Fig. 1(a). A copper tube under test is moved through a Helmholtz-coil-type inducer, which induces an eddy current in the tube by applying the excitation field. In the case of the tube with a flaw, the flaw disturbs the eddy current, and then the disturbed eddy current generates anomalous magnetic signal. An HTS-SQUID gradiometer, which is located at the middle of the field coils forming the Helmholtz-coil-type inducer and above the tube, measures the gradient of the magnetic field generated by the eddy current.

Fig. 1(b) shows the schematic drawing of the SQUID-NDI system cooled using a pulse tube cryocooler (PTC). The system is composed of an HTS-SQUID gradiometer with SQUID electronics, a cryostat with coaxial PTC, Helmholtz-coil-type inducer with position adjuster, a current supplier, a lock-in amplifier, an electric slider with a slider controller and a PC. We employed an HTS-SQUID gradiometer to reduce ambient magnetic noise for operating the system in magnetically unshielding. The gradiometer also contributes to suppress the increase in magnetic noise due to the mechanical vibration by the cryocooler. The HTS-SQUID gradiometer has direct-coupled-type differential rectangular pick-up coils. The dimensions of each pick-up coil and the baseline length of the gradiometer are 2.88 mm × 3.6 mm and 3.6 mm, respectively. We developed a compact coaxial PTC with low mechanical vibration less than 1.5 μm in amplitude at the cold head, which cooled the SQUID down to around 74 K. The details of the gradiometer and PTC are described elsewhere [9,10]. The coaxial PTC with cryostat was set on a nonmetallic and nonmagnetic support. The magnetic flux noise of the SQUID-NDI system measured in a flux-locked loop

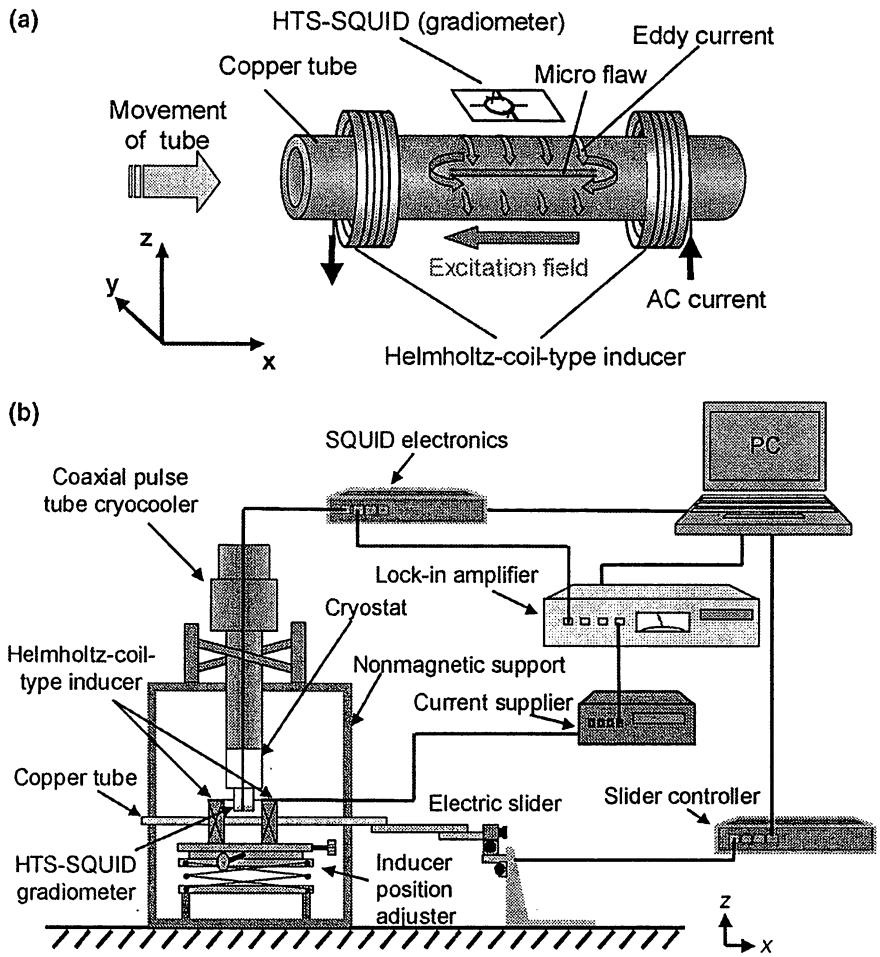

Fig. 1. (a) Principle of the eddy current based SQUID-NDI technique. (b) Schematic diagram of the SQUID-NDI system using a cryocooler.

(FLL) operation without magnetically shielding is about 70 $\mu\phi_0/\mathrm{Hz}^{1/2}$ from 10 Hz to 5 kHz, where $\phi_0 = 2.07 \times 10^{-15}$ Wb is the magnetic flux quantum. Corresponding field gradient noise is about 7 $\mathrm{pT/cm/Hz}^{1/2}$. The Helmholtz-coil-type inducer composes of two field coils. The turn number and dimensions of each field coil are 3000 and 50 mm in diameter and 42 mm in length, respectively. The field coils are placed with a distance of 44 mm between each coil end on the position adjuster while aligning the center of each coil. The electric slider moves the tube through the inducer toward the x-direction. The current supplier gives ac current to the inducer, and also gives a reference signal to the lock-in amplifier. The lock-in amplifier measures the amplitude and phase of the SQUID output. The PC controls the electric slider and obtains the data through the lock-in amplifier.

2.3. Measurements

We demonstrated the inspection of the heat exchanger copper tube specimens with micro-flaws using the SQUID-NDI system. A sinusoidal current of 440 Hz or 5 kHz was supplied to the Helmholtz-coil-type inducer to generate an excitation field. The magnetic flux density B_x was 1.6 μT at the middle of two field coils. The tube specimens were passed stepwise through the inducer with step of 0.3 mm. The flaws were set to be on top of the tube specimens with a lift-off distance 1.5 mm between the HTS-SQUID gradiometer and the top of specimen. The HTS-SQUID gradiometer measured the field gradient in the x-direction of the vertical magnetic field, $\mathrm{d}B_z/\mathrm{d}x$ with the sampling interval space of 0.3 mm. The SQUID output was detected using the lock-in amplifier with a bandwidth of 5 Hz. The position of the inducer

was carefully adjusted relative to the gradiometer before measurements to minimize the SQUID output due to the excitation field itself. The SQUID output due to the excitation field was always set at less than 500 $\mu\phi_0$ (corresponding to 50 pT/cm). However, this output did not affect to the system's sensitivity, because the output was constant during each measurement.

3. Results and discussion

The measurement results on the tube specimens with 100-, 50-, and 30-μm-depth flaws using the excitation field at 440 Hz are shown in Fig. 2(a)–(c). For comparison, measurement result on a *flawless* tube specimen is superposed in Fig. 2(a). In each figure, a cross-sectional view of the tube specimen is depicted below the graph. Fig. 2(a), anomalous signal due to the 100-μm-depth flaw appears above the flaw. The anomalous signals due to the 50- and 30-μm-depth flaws are also observed in Fig. 2(b) and (c), but the signal-to-noise (SN) ratios of these signals are much poorer than that due to the 100-μm-depth flaw. The slantwise variation observed in all results is due to edge effects.

The results of the same specimens with the excitation field at 5 kHz are shown in Fig. 3(a)–(c). With the higher frequency, all anomalous signals due to the flaws were clearly observed. As shown in Fig. 3(c), the 30-μm-depth flaw was successfully detected with an SN ratio of at least 20, where conventional methods should fail to detect. In contrast to Fig. 2, the edge effects are looked to be faint mainly due to the larger longitudinal scaling.

Fig. 4 shows the relationship between the flaw depth and peak–peak amplitude of the field gradient signal due to the flaw obtained from the above-mentioned results. We defined the peak–peak amplitude as shown in Fig. 2(a) with consideration of edge effects, because the field gradient due to edge effects changes approximately linearly as the position changes. In both cases of 440 Hz and 5 kHz excitation, the signal amplitude decreases by a factor of d^2 as flaw depth decreases, where d is the flaw depth [11]. With consideration of this relationship and the system's noise level, the exper-

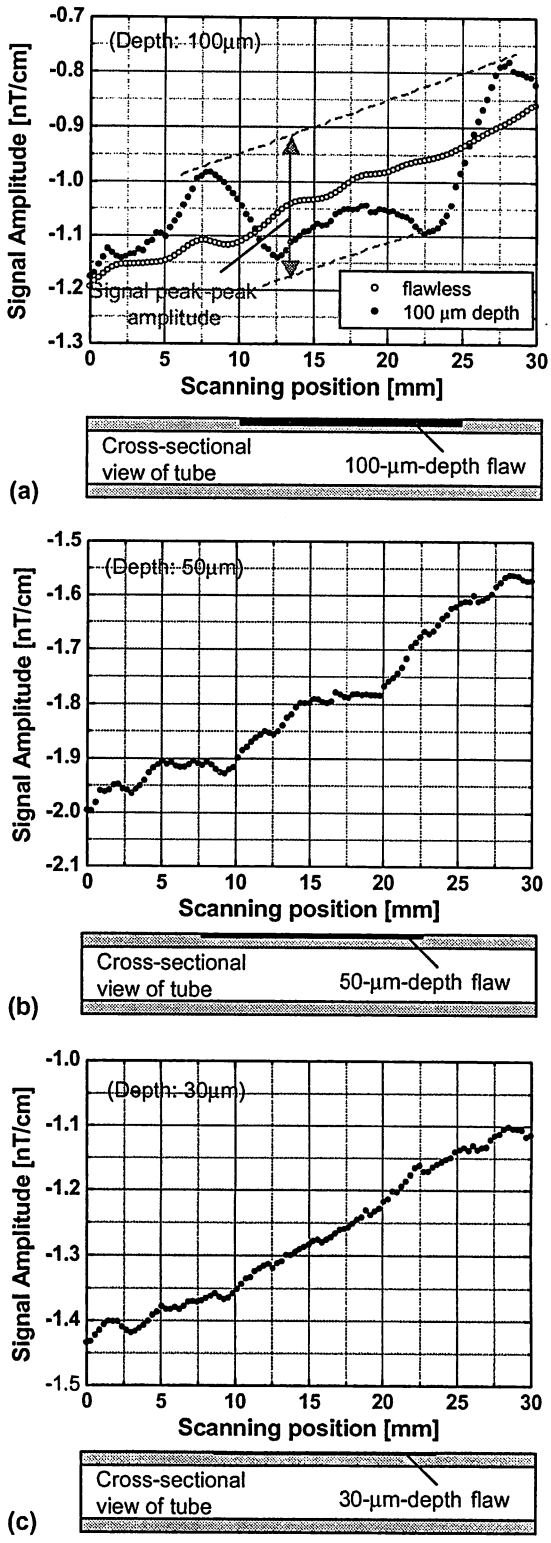

Fig. 2. Measurement results with excitation field of 1.6 μT at 440 Hz. (a) 100-μm-depth flaw, (b) 50-μm-depth flaw, and (c) 30-μm-depth flaw. The result on a flawless specimen is superposed in Fig. (a). The cross-sectional view of the corresponding tube is illustrated below each graph.

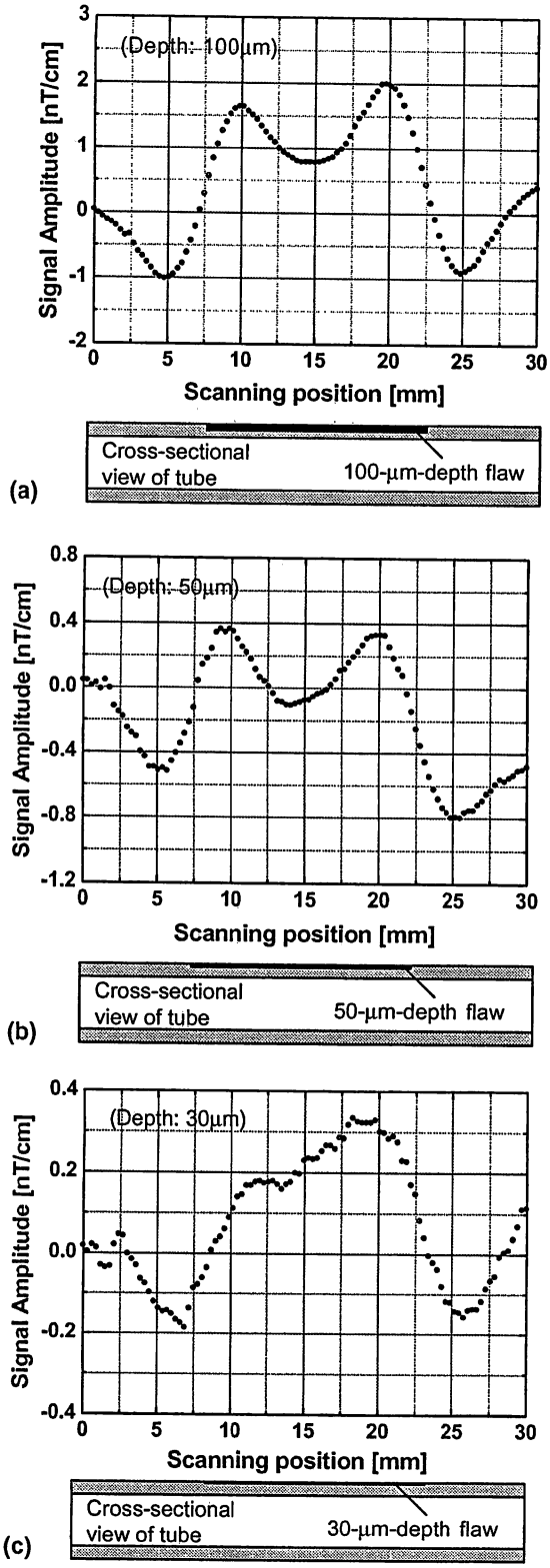

Fig. 3. Measurement results with excitation field of 1.6 μT at 5 kHz. (a) 100-μm-depth flaw, (b) 50-μm-depth flaw, and (c) 30-μm-depth flaw.

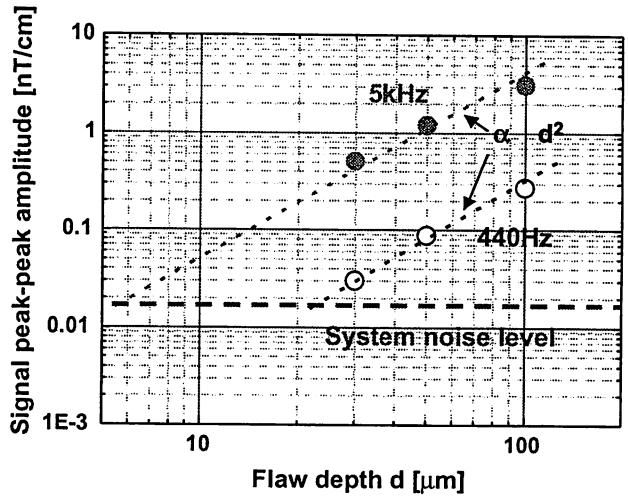

Fig. 4. Relationship between the flaw depth d and the signal peak–peak amplitude due to the flaw.

imental results indicate that the SQUID-NDI system has a potential to detect sub-10-μm-depth flaws.

As shown in Fig. 4, the signal amplitude in 5 kHz excitation is about 13 times larger than that in 440 Hz excitation at the same flaw depth. Accordingly, we experimentally investigated the relationship between the excitation frequency and the signal amplitude. The tube specimen with 30-μm-depth flaw was measured while changing the excitation frequency from 440 Hz to 5 kHz in turn with constant amplitude of excitation field 3.8 μT. Fig. 5 shows the relationship between the excitation frequency and the signal peak–peak amplitude on the specimen. The increase in the signal amplitude with the frequency saturates when the frequency is over 2–3 kHz. In the measurements, we confirmed that the magnitude of the excitation field at each frequency was same, and the sensitivity of the SQUID was constant through the effective bandwidth 10 Hz–5 kHz. Previously, Kondo and Itozaki [12] reported the analogous saturation with this case occurred the in a normal conducting flux transfer coil. They reported that the saturation frequency depended on the resistance and the inductance of the transfer coils. It is supposed that the copper tube played an analogous role with the secondary transfer coil in our case, and then the same kind of saturation occurred. Thus, the saturation frequency may change due to the dimensions of the copper tube and the inducer.

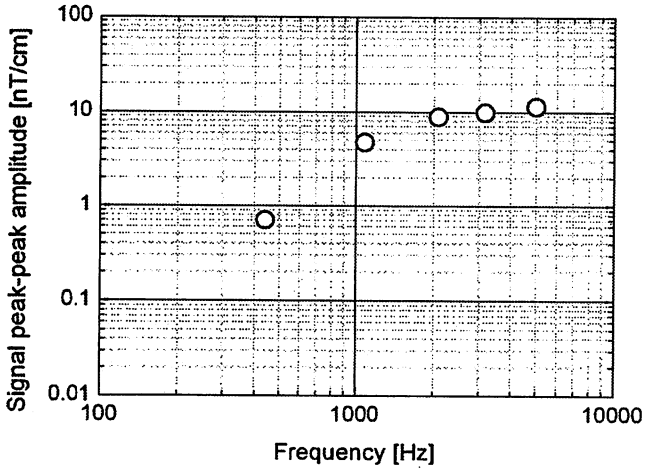

Fig. 5. Relationship between the excitation frequency and the signal peak–peak amplitude due to the 30-μm-depth flaw.

4. Conclusions

We constructed a cryocooler-cooled SQUID-NDI system for the inspection of micro-flaws on heat exchanger copper tubes employing an HTS-SQUID gradiometer and a Helmholtz-coil-type inducer. The detection of artificial flaws several tens of μm in depth was demonstrated using the SQUID-NDI system. With an excitation field of 1.6 μT at 5 kHz, a 30-μm-depth flaw was successfully detected at an SN ratio of about 20. The signal peak–peak amplitude of the signal due to the flaw is in proportion to the square of flaw depth. With consideration of the system's noise level, the results indicate that sub-10-μm-depth flaws are detectable using the SQUID-NDI system. The measures against the high-speed transfer of the tubes and the vibration of tubes due to the high-speed transfer will be taken for the commercial use in an actual tube factory.

Acknowledgement

The authors gratefully acknowledge helpful discussions with N. Kasai at National Institute of Advanced Industrial Science and Technology (AIST).

References

[1] A.J. Trivedi, R.R. Parikh, in: Proc. 14th World Conf. Non-Destructive Testing, vol. 3, 1996, p. 1729.
[2] K.A. Gopal, N. Raghu, N.G. Muralidharan, P.V. Kumar, K.V. Kasiviswanathan, in: Proc. 14th World Conf. Non-Destructive Testing, vol. 2, 1996, p. 663.
[3] A. Fedorov, V. Popov, V. Gorsky, A.A. Bochvar, in: Proc. 14th World Conf. Non-Destructive Testing, vol. 3, 1996, p. 1709.
[4] A. Barone (Ed.), Principle and Application of Superconducting Quantum Interference Devices, World Scientific, Singapore, 1992, p. 64.
[5] D. Lesselier, A. Razek (Eds.), Studies in Applied Electromagnetics and Mechanics, vol. 15, IOS Press, Amsterdam, 1999, p. 159.
[6] M. Valentino, A. Ruosi, G. Pepe, V. Mollo, R. D'Alto, G. Peluso, Int. J. Mod. Phys. B 13 (1999) 1117.
[7] H.-J. Krause, M.V. Kreutzbruck, Physica C 368 (2002) 70.
[8] S. Tanaka, T. Mizoguchi, H. Ota, Y. Kondo, IEICE Trans. Electron E85-C (2002) 687.
[9] Y. Hatsukade, T. Inaba, N. Kasai, Y. Maruno, A. Ishiyama, S. Tanaka, Physica C 412–414 (2004) 1484.
[10] Y. Hatsukade, N. Kasai, H. Takashima, A. Sakamaki, Y. Maruno, S. Tanaka, A. Ishiyama, Submitted to EUCAS 2003 Proc.
[11] Y. Hatsukade, A. Kosugi, K. Mori, S. Tanaka, Jpn. J. Appl. Phys. 43 (2004) L1488.
[12] T. Kondo, H. Itozaki, Supercond. Sci. Technol. 17 (2004) 459.